Article

UDC 621.762:539.2

https://doi.org/10.31489/2026PH2/38-48

Received: 02.02.2026
Accepted: 10.04.2026

S.A. Ghyngazov[1], I.P. Vasil'ev[1], V.A. Boltueva[1],
S. Bobuyok[1], I.K. Chakin[2], V.P. Krivobokov[1]

[1]*National Research Tomsk Polytechnic University, Tomsk, Russia;*
[2]*Budker Institute of Nuclear Physics, Novosibirsk, Russia*

The Influence of Electron Processing of the Powder Mixture of Initial Reagents on the Sintering of High-Entropy Ceramics $(Ca_{0.2}Sr_{0.2}Ba_{0.2}Pb_{0.2}La_{0.2})TiO_3$

The development of thermoelectric materials has attracted considerable attention with the emergence of a new class of high-entropy materials. Their fabrication is typically based on solid-state synthesis and involves prolonged mechanical mixing of powder precursors, high-temperature heat treatment, and multiple repetitions of these operations. The paper addresses the issues of accelerating the manufacturing process of highly entropic ceramics for thermoelectric applications through the use of electron beam processing. The effect of cyclic processing of a powder mixture of initial reagents in air with a high-energy electron beam (E = 1.4 MeV) on the sintering of compacts was studied using high-entropy perovskite ceramics $(Ca_{0.2}Sr_{0.2}Ba_{0.2}Pb_{0.2}La_{0.2})TiO_3$ as an example. The electron beam current was 4 mA (5 treatment cycles) and 5 mA (4 treatment cycles), with mechanical grinding of the powder after each irradiation step. It was found that electron beam treatment enhances the compaction/sintering kinetics. The efficiency of the treatment increases with the number of cycles. As a result, the sintering process is accelerated, leading to increased ceramic density and mechanical strength. These improvements are attributed to the formation of the high-entropy phase $(Ca_{0.2}Sr_{0.2}Ba_{0.2}Pb_{0.2}La_{0.2})TiO_3$ in the powder mixture as a result of electron beam processing.

Keywords: high-entropy ceramics, perovskites, synthesis, electron beams, sintering

✉*Corresponding author*: Ghyngazov, Sergei, ghyngazov@tpu.ru

Introduction

The development of solar energy is largely associated with perovskites [1]. The most well-known representative of this class of materials is calcium titanate ($CaTiO_3$), which is widespread in nature, readily available, and inexpensive [2]. Perovskite solar cells are considered the basis for tandem (e.g., perovskite-silicon) cells, which could significantly increase the efficiency of solar panels and make solar energy more accessible. One of the main drawbacks of conventional perovskites is their instability at high temperatures [3]. Perovskite materials, especially those based on lead methylammonium iodide, tend to degrade rapidly when exposed to moisture, oxygen, high temperatures, and intense sunlight [4]. This leads to the destruction of their crystal structure and a loss of efficiency, making them less durable compared to traditional silicon solar cells. For example, modern silicon panels lose about 0.5 % of their power per year, while perovskite cells can lose up to 10 % of their power in just two months of operation. An integrated approach—a combination of defect engineering, composition modification, surface protection, and encapsulation—can significantly improve the efficiency, stability, and environmental safety of perovskite solar cells, bringing them closer to mass commercial use. However, these measures do not completely solve the problem. New prospects for improving the properties of perovskites have emerged with the development of high-entropy ceramics. The concept of creating a high-entropy state was first successfully implemented in alloys [5]. Outstanding achievements in producing alloys with unique properties have stimulated research into the creation of high-entropy ceramics [6]. High-entropy ceramics (HECs) are materials composed of five or more elements that form a homogeneous crystalline structure. Due to their unique combination of properties, such as high thermal stability, wear resistance, low thermal conductivity, high strength, and permittivity, they find application in a wide range of fields. In aerospace engineering, HECs are used as thermal barrier coatings and structural components for operation under ultra-high temperatures and loads, for example, in engines, nozzles, and thermal protection systems [7]. In the energy industry, they are employed in the manufacture of solid oxide fuel cell components, high-temperature insulation materials [8], and energy storage systems [9]. Additionally, HECs

and their oxides serve as catalysts for chemical reactions, including those involved in energy purification and conversion processes. Transparent high-entropy ceramics can be used as protective coatings for optics, screens, and semiconductor devices due to their plasma resistance and low etching rate [10]. The properties of thermoelectric materials have been improved thanks to the development of high-entropy perovskites [11]. These materials constitute a new class of compounds whose crystal structure contains five or more different elements in approximately equal proportions in one or both cationic sublattices. This composition provides high configurational entropy, which stabilizes the structure and imparts unique properties. Therefore, the synthesis and sintering of high-entropy perovskite materials has become a particularly pressing issue. The technology for synthesizing high-entropy perovskites typically involves the following basic steps, which form the basis of solid-phase synthesis [12, 13]. Initially, the starting oxide powders are mechanically mixed in a stoichiometric ratio using a planetary ball mill. The powder mixture is then fired and reground in the mill; this process may be repeated several times to ensure homogeneity. After milling, the dispersed powders are used to form compacts of a given shape (green bodies). The ceramics are subsequently sintered from these compacts, followed by prolonged annealing of the ceramic billets at high temperature in an inert atmosphere. This annealing step enhances the conductive properties of the material, which is essential for its performance as a thermoelectric. As can be seen from the above, the fabrication process for thermoelectric materials is very time-consuming and expensive. These drawbacks can be significantly mitigated by accelerating the synthesis and improving the quality of the sintering process. In this work, it is proposed to activate these processes by treating the initial powder mixture of reagents with a powerful beam of high-energy electrons. One of the known methods for activating the sintering of powder compacts is the pretreatment of powders by electron irradiation [14, 15]. Electron treatment of powders is usually carried out in a vacuum, which complicates the technological process. Currently, electron accelerators are available that allow the extraction of electron beams with energies of 1 MeV or more into the air atmosphere [16, 17]. Using such electron beams makes it possible to process powder systems in air with high speed and efficiency [18, 19].

In this work, for the first time, the effect of high-energy electron beam treatment in an air atmosphere on the shrinkage kinetics of compacts made from a powder mixture of initial reagents is investigated.

Materials and Methods

Commercial powders of $CaTiO_3$, $SrTiO_3$, $BaTiO_3$, $PbTiO_3$, La_2O_3, and TiO_2 with a purity of 99.99 % were used as starting materials for the synthesis of high-entropy ceramics with the composition $(Ca_{0.2}Sr_{0.2}Ba_{0.2}Pb_{0.2}La_{0.2})TiO_3$. Simultaneous thermal analysis of these powders was performed using an STA 449 device (Netzsch, Germany). To maintain the specified stoichiometry of the resulting ceramics, a powder mixture was prepared in the molar ratio $4CaTiO_3 + 4SrTiO_3 + 4BaTiO_3 + 4PbTiO_3 + 2La_2O_3 + 4TiO_2$. Mixing of the powders was carried out in a humid environment using a Tencan XQM-2A planetary ball mill. The mixture was then dried in a resistance furnace at a temperature of 150 °C for 2 hours. Part of the powder mixture prepared in this way was left in its original state, while the remaining part was divided into portions and subjected to short-term treatment with high-energy electrons in air using an electron accelerator (Unique scientific installation “Stand ELV-6”, INP SB RAS, Novosibirsk, Russia). The ELV-6 Stand and the electron beam processing technique are described in detail in [20, 21]. The issues of the formation of temperature fields in powder samples, the distribution of energy density, and the depth of electron penetration were previously discussed in detail in [22]. Powder compacts for sintering high-entropy ceramics were obtained by uniaxial pressing on a PGR-10 press at a pressure of 100 MPa. Sintering of $(Ca_{0.2}Sr_{0.2}Ba_{0.2}Pb_{0.2}La_{0.2})TiO_3$ ceramic samples was carried out in air within the furnace chamber of a DIL 402 C dilatometer (Netzsch, Germany) at a temperature of 1200 °C for 5 hours. The heating and cooling rates were 10 °C/min. After electron beam processing at beam currents of 4 mA and 5 mA, the powder was mechanically ground in an agate mortar. The resulting powder was then placed into a massive copper die and again subjected to electron beam processing under identical conditions. This sequence of actions was repeated five times for a current of 4 mA and four times for a current of 5 mA. After each electron beam exposure, a powder sample was taken for the production of powder compacts. To obtain reliable results, all experiments were carried out repeatedly in the amount of at least three.

Results and Discussion

Figure 1 shows the TG and DSC curves for each individual powder (TiO_2, La_2O_3, $BaTiO_3$, $SrTiO_3$, $CaTiO_3$, $PbTiO_3$) included in the powder mixture.

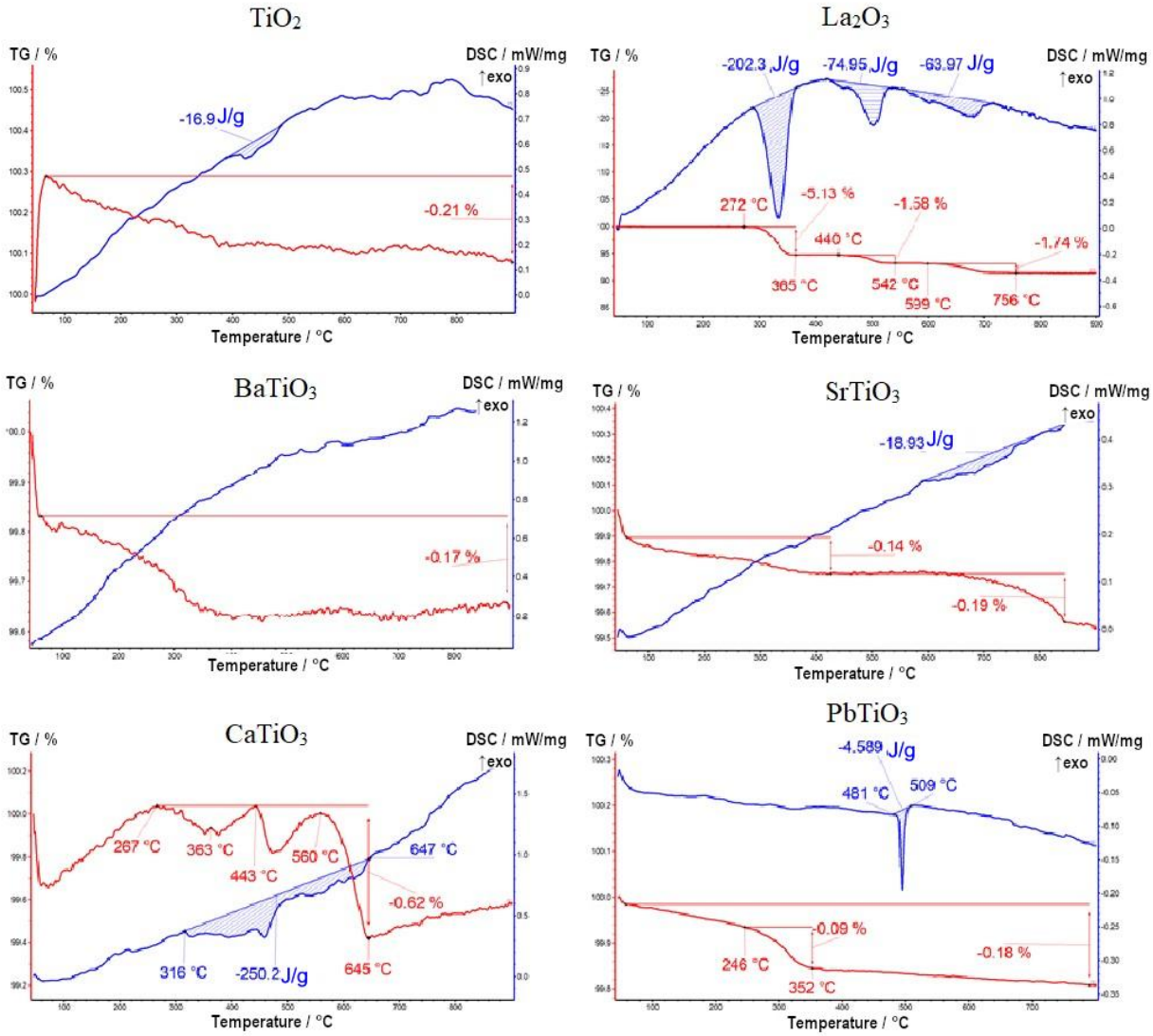

Figure 1. TG and DSC curves for the initial powders used in the synthesis of high-entropy ceramics $(Ca_{0.2}Sr_{0.2}Ba_{0.2}Pb_{0.2}La_{0.2})TiO_3$

Figure 1 shows that for all components of the reaction mixture, except for La_2O_3, the weight loss is less than 1 % and is primarily due to the desorption of adsorbed water. At temperatures below 100 °C, a slight weight loss is observed, which is attributed to the desorption of physically bound water. In the temperature range of 100–500 °C, the removal of loosely bound moisture occurs. For La_2O_3, more significant weight changes are observed, which may be due to its tendency to interact with carbon dioxide and water from the atmosphere via the following mechanism.

$$La_2O_3 + 2CO_2 + H_2O \rightarrow 2LaCO_3(OH).$$

Upon heating, hydroxyl groups are initially eliminated with the release of a water molecule. As the temperature increases further, decarboxylation of the residual carbonate occurs, accompanied by the evolution of carbon dioxide. The overall decomposition process of lanthanum hydroxycarbonate is expressed by the equation:

$$2LaCO_3(OH) \rightarrow La_2O_3 + CO_2 + H_2O.$$

Since the weight loss during heating of the La_2O_3 powder (Fig. 1) is several times greater than that of each of the other powders in the reaction mixture, the shape of the TG and DSC curves for the mixture of initial reagents completely repeats the corresponding curves for pure La_2O_3 powder (Fig. 2).

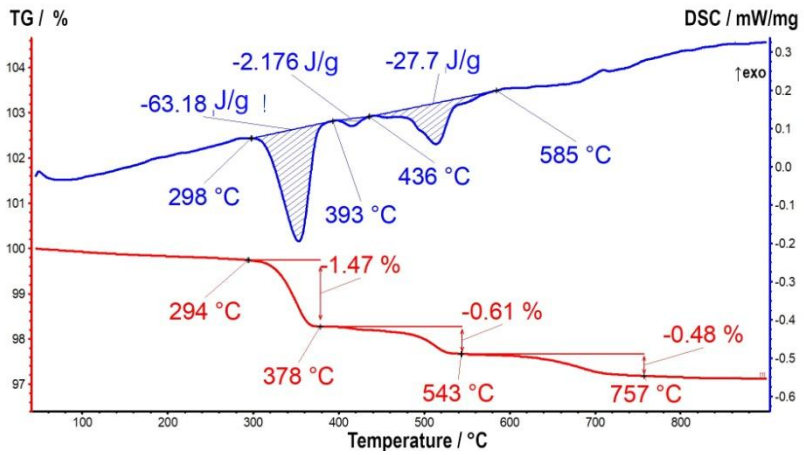

Figure 2. TG and DSC curves for the powder mixture in the molar ratio:
$4CaTiO_3 + 4SrTiO_3 + 4BaTiO_3 + 4PbTiO_3 + 2La_2O_3 + 4TiO_2$

Figure 2 shows the results of TG and DSC analysis for a powder mixture of complex composition: $4CaTiO_3 + 4SrTiO_3 + 4BaTiO_3 + 4PbTiO_3 + 2La_2O_3 + 4TiO_2$. According to the TG data, the slight weight loss observed at temperatures below 100 °C is associated with the removal of physically adsorbed moisture from the surface of the powder particles. The sharp decrease in weight in the temperature range of 300–360 °C is mainly due, as described above, to the weight loss of lanthanum oxide present in the powder mixture as a result of the release of H_2O and CO_2. A less pronounced weight loss in the temperature range of 400–600 °C can be explained by the combustion of residual organic matter and the removal of residual moisture. The occurrence of these processes is confirmed by the presence of corresponding endothermic peaks on the DSC curve (Fig. 2). Thus, the results of simultaneous thermal analysis demonstrate that, upon heating the powder mixture to the sintering temperature, no decomposition of the titanates occurs. The minor weight loss observed is attributed to the release of previously adsorbed moisture and the products of the decomposition of lanthanum hydroxycarbonate and lanthanum oxide. This result confirms literature data on the high-temperature stability of all selected reagents.

Figure 3 shows photographs of a massive copper container holding a powder mixture before (Fig. 3*a*) and after treatment with a 1.4 MeV electron beam (Fig. 3*b* and 3*c*). The electron beam current was 4 mA, and the container moved under the beam at a speed of 1 cm/s. The beam itself was scanned across the internal width of the container at a frequency of 50 Hz.

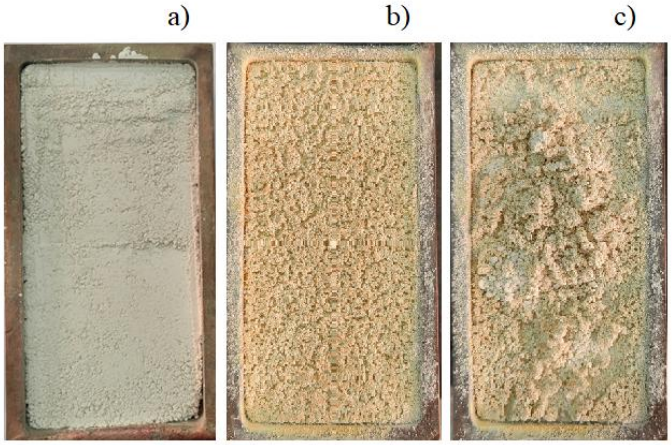

Figure 3. Photographs of the container before (*a*) and after (*b*, *c*) treatment with a 1.4 MeV electron beam. Beam current: 4 mA; container movement speed under the beam: 1 cm/s

Figure 3*c* shows the structure within the irradiated powder layer (part of the powder was swept toward the center of the container). It is evident that, as a result of brief electron-beam heating, the powder mixture changed color, and the powder grains entered into solid-phase interactions with each other. This is evidenced

by the formation of a highly porous plate (Fig. 3*b*), which readily disintegrates into large particles in the form of agglomerates of smaller particles (Fig. 3*c*). The absence of melting droplets in the electron-treated powder (Figs. 3*b* and 3*c*) indicates that the temperature of the powder mixture did not reach the melting point of any of its components during electron-beam heating. The mechanical adhesion of the powder particles indicates that interparticle solid-phase interactions occurred. SEM images of the powder mixture particles and EDS spectra of the main elements of the powder particles after the first and fourth irradiation/grinding cycles are shown in Figure 4 and Figure 5, respectively. The treatment included electron beam irradiation at E = 1.4 MeV, beam current I = 5 mA, scan speed V = 1 cm/s, and subsequent grinding in an agate mortar.

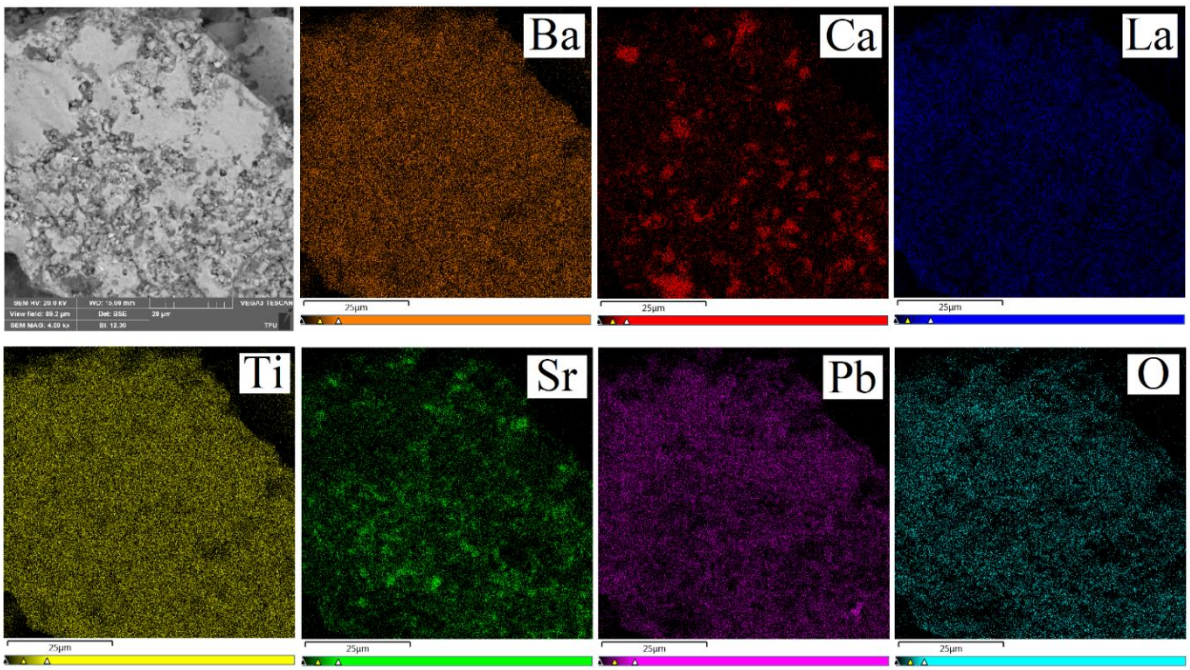

Figure 4. SEM image of a powder mixture particle and the corresponding EDS spectrum of the main elements after the first processing cycle (E = 1.4 MeV, I = 5 mA, V = 1 cm/s)

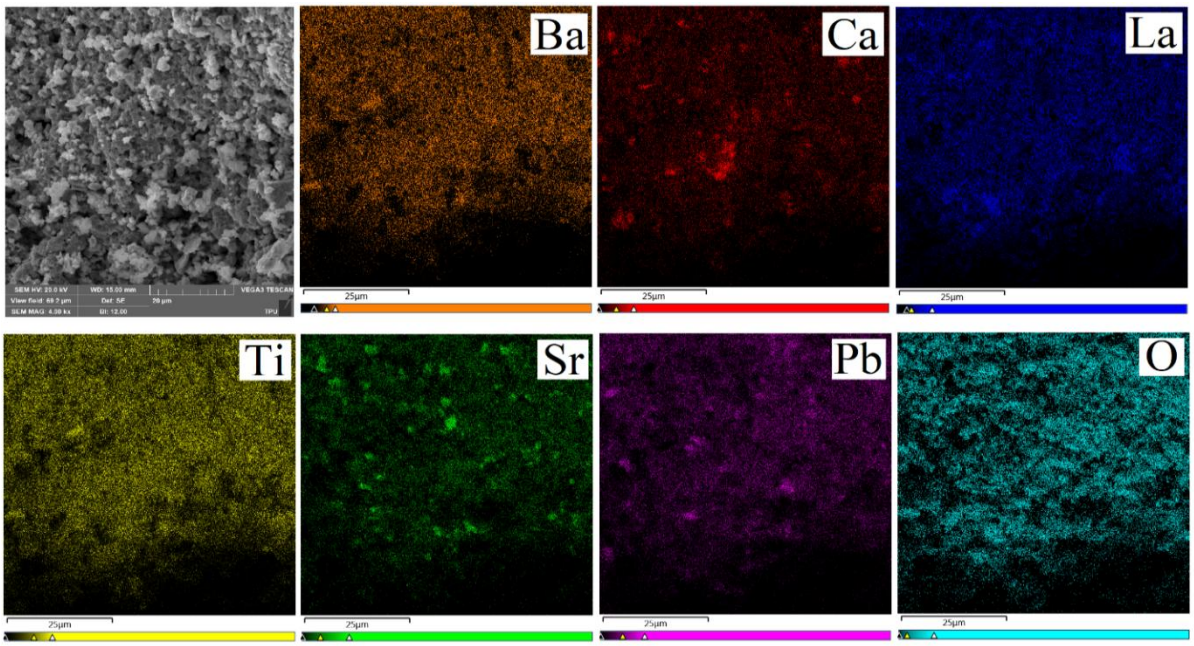

Figure 5. SEM image of a powder mixture particle and the corresponding EDS spectrum of the main elements after the fourth processing cycle (E = 1.4 MeV, I = 5 mA, V = 1 cm/s)

The SEM image in Figure 4 shows that after a single short-term exposure to the electron beam, the mixture consists of particle agglomerates, and the agglomerate surface is partially melted. The occurrence of solid-phase interparticle interaction during a single treatment can be judged from the analysis of the XRD data presented in Figure 6. For a beam current of 5 mA, the diffraction pattern has a shape corresponding to ceramics of the composition $(Ca_{0.2}Sr_{0.2}Ba_{0.2}Pb_{0.2}La_{0.2})TiO_3$ [22]. The data in Figure 5 indicate a change in the structure of the mixture particles after four irradiation cycles with an electron beam at $I = 5$ mA. The SEM image of the particles is typical of sintered ceramics. The distribution of the main elements by volume for all elements except Ca and Sr is characterized by high uniformity. The X-ray diffraction results are shown in Figure 6. The clean sharp peaks for samples sintered from electron-untreated powders indicate that a homogeneous phase was formed due to atomic diffusion over a period of 5 hours. Figure 6 also shows that the same type of diffraction pattern is recorded in the powder mixture after a single treatment with an electron beam with a current of 5 mA. During the analysis, a comparison with the peaks of cubic perovskite $CaTiO_3$ (PDF#43-0226) and $SrTiO_3$ (PDF#35-0734) was used. The calculated value of the lattice parameter a is 3.915 Å, indicating that that the larger Ba, Pb, and La atoms occupied the A-position of perovskite, which led to an expansion of the lattice, which is typical for the high-entropy phase. After repeated electronic processing (upper diffractogram), peak splitting is observed, which, according to [22], is explained by oxygen deficiency due to a partial decrease in Ti^{4+} to Ti^{3+}.

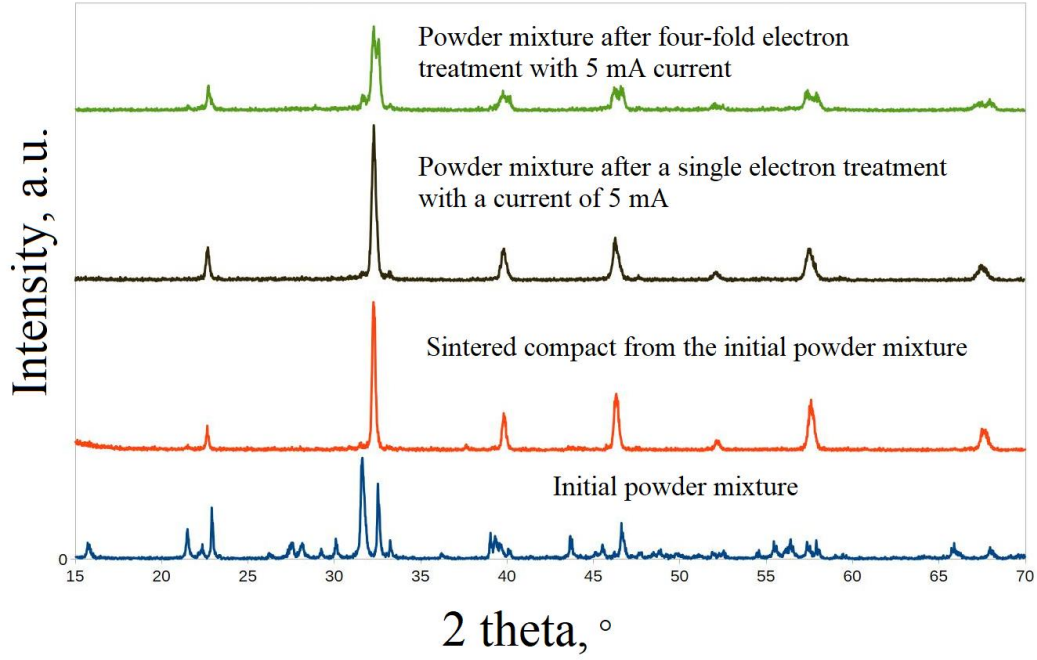

Figure 6. XRD patterns of the initial powder mixture, the compact sintered from it, and the initial powder after single and quadruple electron beam treatment. Electron energy: 1.4 MeV; beam current: 5 mA; cuvette movement speed under the beam: 1 cm/s

Thus, the presented experimental data indicate that preliminary short-term electron beam treatment of the powder mixture with the composition $4CaTiO_3 + 4SrTiO_3 + 4BaTiO_3 + 4PbTiO_3 + 2La_2O_3 + 4TiO_2$ initiates the synthesis of ceramics with the composition $(Ca_{0.2}Sr_{0.2}Ba_{0.2}Pb_{0.2}La_{0.2})TiO_3$ within the bulk of the mixture. With an increase in the number of irradiation/grinding cycles, the yield of the synthesized product increases, and the powder particles obtained after multiple treatments exhibit a ceramic nature. The results of dilatometry are presented in Figures 6–8.

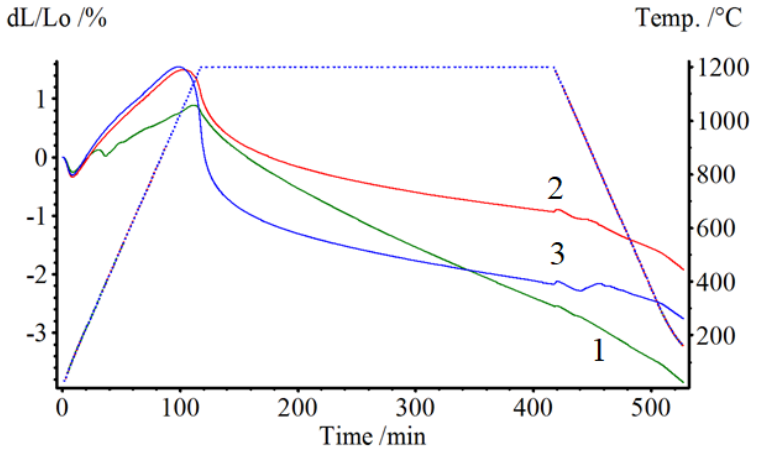

Figure 6. Dilatometric analysis of compacts for the sintering of $(Ca_{0.2}Sr_{0.2}Ba_{0.2}Pb_{0.2}La_{0.2})TiO_3$ ceramics from a powder mixture: (*1*) before treatment, (*2*) after a single treatment with a high-power electron beam, and (*3*) after five treatments with intermediate milling. Electron energy: 1.4 MeV; beam current: 4 mA; cuvette movement speed under the beam: 1 cm/s

The dilatograms (shrinkage curves) in Figure 6 show that the compact made from the initial powder mixture, when heated from 300 to 400 °C, exhibits a region of compaction followed by expansion, despite an overall tendency toward shrinkage. This behavior can be attributed to moisture release processes, as shown in Figure 2 (the position of the endothermic peak on the DSC curve). During isothermal holding, the compact steadily compacts, and during the cooling stage, at a temperature of approximately 300 °C, a region of barely noticeable abrupt change in linear dimension is observed, which is usually associated with a phase transition in the material under study.

The dilatograms for compacts (Fig. 6, curves *2* and *3*) obtained from powder mixtures subjected to electron beam treatment do not exhibit any changes in linear dimensions during the heating stage, unlike those for the compact from the initial powder mixture. The increase in linear dimensions during heating is more pronounced. The shrinkage curves themselves have a shape characteristic of ceramic sintering: the compact expands during heating, and when the temperature reaches 900–1000 °C, compaction processes begin to prevail over linear expansion, with the maximum shrinkage rate observed upon reaching the sintering temperature. As the heating time increases, the shrinkage rate decreases, indicating the formation of the ceramic structure of the sample. Increasing the electron beam current to 5 mA during the initial processing further enhances compaction (Fig. 7, curve *2*).

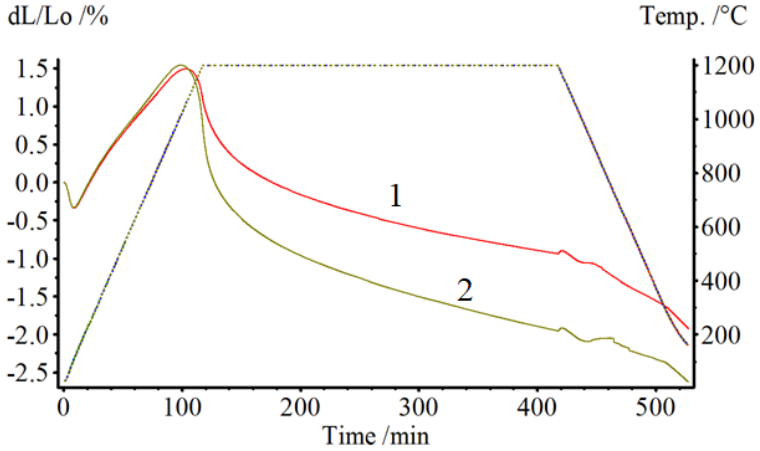

Figure 7. Dilatometric analysis of compacts for the sintering of $(Ca_{0.2}Sr_{0.2}Ba_{0.2}Pb_{0.2}La_{0.2})TiO_3$ ceramics from a powder mixture after a single treatment with a high-power electron beam (E = 1.4 MeV; scan speed: 1 cm/s): Curve 1 — beam current 4 mA; Curve 2 — beam current 5 mA

The trends observed for the effect of electron beam current on the shrinkage of powder compacts after a single electron beam treatment are preserved for multiple irradiation/grinding cycles (Fig. 8).

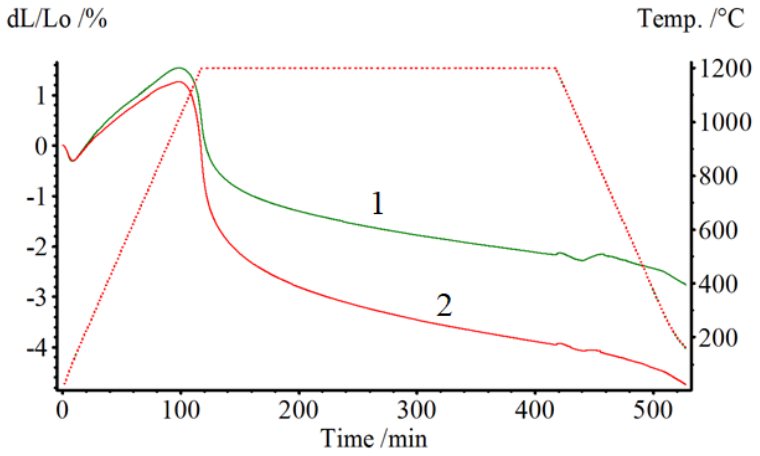

Figure 8. Dilatometric analysis of compacts for the sintering of $(Ca_{0.2}Sr_{0.2}Ba_{0.2}Pb_{0.2}La_{0.2})TiO_3$ ceramics from a powder mixture after multiple treatments with a high-power electron beam (E = 1.4 MeV; scan speed: 1 cm/s): Curve 1 — 5 treatment cycles at a beam current of 4 mA; Curve 2 — 4 treatment cycles at a beam current of 5 mA

Figure 8 shows that the shrinkage of the compacts increases with repeated electron beam processing. This effect is most pronounced at an electron beam current of 5 mA. Moreover, the change in linear dimension during the cooling stage is minimal in this case, which can be explained by the formation of a stable, high-entropy state in the sintered ceramics. These observed shrinkage patterns are confirmed by density measurements of the sintered ceramic samples, presented in Table 1.

Table 1

Measurement results for the density, porosity, and hardness of ceramic samples of $(Ca_{0.2}Sr_{0.2}Ba_{0.2}Pb_{0.2}La_{0.2})TiO_3$. Thermal sintering: 1200 °C, 5 hours

Compact type	Density, g/cm^3	Open porosity, %	Hardness, GPa
The compacts were fabricated from the as-prepared powder mixture	3.27±0.32	41±6	2.75±0.21
From the powder after a single electron beam treatment at a beam current of 4 mA	4.40±0.28	20±4	3.2±0.32
From the powder after four cycles of electron beam treatment at a beam current of 5 mA	5.04±0.36	8±1	6.11±0.33

The data in Table 1 indicate an increase in the density and hardness of the sintered ceramics after electron beam treatment of the initial powder mixture, accompanied by a corresponding decrease in open porosity. The low density and high porosity of the ceramics sintered from the initial powder mixture, which was not subjected to electron beam treatment, indicate that the sintering time was insufficient. The change in the compact shrinkage kinetics after electron beam treatment can be explained based on the X-ray diffraction data presented in Figure 6. The diffraction pattern for the ceramics sintered from the initial powder mixture indicates incomplete formation of the high-entropy phase and contains a small number of extraneous peaks. Their presence is evidence of incomplete synthesis during sintering. With an increasing number of electron beam treatments, the content of the high-entropy phase in the powder mixture increases. Compacts formed from powders with a high content of the high-entropy phase are compacted more efficiently, since the synthesis processes that hinder ceramic compaction are partially or completely completed under the influence of the electron beam. Powder subjected to multiple electron beam treatments is characterized by a diffraction pattern that most closely matches the samples obtained in [22]. Thus, as the number of irradiation treatments increased, the sintering behavior of compacts made from treated powders became similar to that of ceramics where particle compaction is the primary mechanism. Moreover, thermal energy is not wasted on material synthesis. Consequently, preliminary electron beam treatment of the powder mixture allows for a significant reduction in the sintering time of ceramic products. Electron beam treatment significantly accelerates synthesis and, accordingly, reduces the time and cost of ceramic production.

Conclusion

Using the example of high-entropy ceramics $(Ca_{0.2}Sr_{0.2}Ba_{0.2}Pb_{0.2}La_{0.2})TiO_3$, a promising material for solar energy applications, we studied the effect of treatment in air with high-energy electrons (1.4 MeV) on the synthesis and sintering of this ceramic. It was found that, starting from the first cycle of short-term electron beam treatment, the radiation processing is accompanied by the formation of the oxides constituting the high-entropy phase $(Ca_{0.2}Sr_{0.2}Ba_{0.2}Pb_{0.2}La_{0.2})TiO_3$ in the powder mixture. With an increasing number of treatment/grinding cycles, the phase composition of the mixture increasingly corresponds to that of the target $(Ca_{0.2}Sr_{0.2}Ba_{0.2}Pb_{0.2}La_{0.2})TiO_3$ ceramics. The effectiveness of the treatment increases with the number of cycles, which accelerates the sintering process and leads to an increase in the ceramic's density and mechanical strength.

Acknowledgment

This work was supported by the Russian Science Foundation [grant no. 23-79-00014].

References

1 Wang, R., Zhang, J., Cao, Y., ... Liu, S., & Feng, J. (2026). Reconstruction of the surface for efficient 3D/quasi-2D heterostructured inverted perovskite solar cells. *Advanced Functional Materials*, *36*(15), e17633. DOI: 10.1002/adfm.202517633.

2 Gralik, G., Thomsen, A.E., Moraes, C.A., Raupp-Pereira, F., & Hotza, D. (2014). Processing and characterization of $CaTiO_3$ perovskite ceramics. *Processing and Application of Ceramics, 8*(2), 87–92. DOI: 10.2298/PAC1402053G.

3 Wan, Z., Wei, R., Zhao, H., ... Luo, J., & Jia, C. (2026). Thermal management technologies for improving the thermal stability of perovskite solar cells. *NanoMicroLetters, 18*(1), 207. DOI: 10.1007/s40820-025-02047-x.

4 Reddy, D.J., & Lazarus, I.J. (2024). Fabrication and characterization of methylammonium lead iodide-based perovskite solar cells under ambient conditions. *Indonesian Journal of Electrical Engineering and Computer Science, 34*(3), 1410–1419. DOI: 10.11591/ijeecs.v34.i3.pp1410-1419.

5 Salifu, S., & Olubambi, P.A. (2025). High entropy alloy reinforced lightweight metal matrix composites: A review of the fundamentals, fabrication, properties, and prospects. *Materials Today Sustainability,* 32, 101216. DOI: 10.1016/j.mtsust.2025.101216.

6 Zhang, R.-Z., & Reece, M.J. (2019). Review of high entropy ceramics: design, synthesis, structure and properties. *Journal of Materials Chemistry A, 7*(39), 22148–22162. DOI: 10.1039/c9ta05698j.

7 Wang, M., Liu, R., Qi, K., ... Li, Z., & Sun, C. (2025). Research progress of high-temperature resistant aerogel thermal insulation materials for aerospace applications. *Journal of Ceramics, 46*(4), 672–688. DOI: 10.13957/j.cnki.tcxb.2025.04.003.

8 Sharma, Y., Mazza, A.R., Musico, B.L., ... Keppens, V., & Ward, T.Z. (2021). Magnetic texture in insulating single crystal high entropy oxide spinel films. *ACS Applied Materials and Interfaces, 13*(15), 17971–17977. DOI: 10.1021/acsami.1c01344.

9 Sun, L., Wang, J., Hu, Z., Chen, W., & Sun, C. (2026). Advances in high-entropy oxides for reversible protonic ceramic cells applications. *Applied Energy, 411*, 127595. DOI: 10.1016/j.apenergy.2026.127595.

10 Wang, B., Hao, Y., Xu, Y., Chen, X., & Zhang, K. (2026). Investigation on the microstructure, optical, and mechanical properties of multi-component sesquioxide transparent ceramics. *Journal of the European Ceramic Society, 46*(5), 118017. DOI: 10.1016/j.jeurceramsoc.2025.118017.

11 Jiang, S., Hu, T., Gild, J., ... Vecchio, K., & Luo, J. (2018). A new class of high-entropy perovskite oxides. *Scripta Materialia, 142*, 116–120. DOI: 10.1016/j.scriptamat.2017.08.040.

12 Vinnik, D.A., Trofimov, E.A., Zhivulin, V.E., ... Trukhanov, S.V., & Podgornov, F.V. (2020). High entropy oxide phases with perovskite structure. *Nanomaterials, 10*(2), 268. DOI: 10.3390/nano10020268.

13 Li, S., Li, J., Zhou, C., ... Yan, J., & Qi, X. (2022). Research on the dielectric energy storage characteristics of the $[(Bi_{0.5}Na_{0.5})_{0.2}Ba_{0.2}Sr_{0.2}Ca_{0.2}Mg_{0.2}]TiO_3$ equal ratio high-entropy ceramics. *Journal of Materials Science Materials in Electronics, 33*(30), 23792–23805. DOI: 10.1007/s10854-022-09137-1.

14 Il'in, A.P., Root, L.O., & Mostovshchikov, A.V. (2012). The rise of energy accumulated in metal nanopowders. *Technical Physics, 57*(8), 1178–1180. DOI: 10.1134/S1063784212080129.

15 Mostovshchikov, A.V., Ilyin, A.P., & Egorov, I.S. (2024). Effect of electron beam irradiation on the thermal properties of the aluminum nanopowder. *Radiation Physics and Chemistry, 153*, 156–158. DOI: 10.1016/j.radphyschem.2018.09.024.

16 Fadeev, S.N., Golkovski, M.G., Korchagin, A.I., ... Salimov, R.A., & Vaisman, A.F. (2000). Technological applications of BINP industrial electron accelerators with focused beam extracted into atmosphere. *Radiation Physics and Chemistry, 57*(3–6), 653–655. DOI: 10.1016/S0969-806X(99)00499-5.

17 Vorobev, D.S., Domarov, E.V., Golkovskii, M.G., ... Lavrukhin, A.V., & Nemytov, P.I. (2021). Accelerators of ELV series: current status and further development. *CERN Proceedings,* 111–113. DOI: 10.18429/JACoW-RuPAC2021-FRB02.

18 Ghyngazov, S.A., Surzhikov, A.P., Vasil'ev, I.P., Boltueva, V.A., & Vlasov, V.A. (2024). Synthesis of high-entropy ceramics $(Y_{0.2}Yb_{0.2}Lu_{0.2}Eu_{0.2}Er_{0.2})_3Al_5O_{12}$ by electron beam heating. *Ceramics International, 50*(22), 45037–45043. DOI: 10.1016/j.ceramint.2024.08.342.

19 Ghyngazov, S.A., Vasil'ev, I.P., Boltueva, V.A., & Vlasov, V.A. (2025). Electron beam synthesis of $CaZrTi_2O_7$ zirconolite ceramics. *Russian Physics Journal, 68*(9), 1454–1458. DOI: 10.1007/s11182-025-03580-3.

20 Ghyngazov, S.A., Boltueva, V.A., & Vasil'ev, I.P. (2024). Synthesis of oxide ceramics in a beam of fast electrons. *Bulletin of the University of Karaganda – Physics*, *29*(4(116)), 27–34. DOI: 10.31489/2024/PH4/27-34.

21 Golkovski, M.G., Denisov, I.P., Ghyngazov, S.A., Vasil'ev, I.P., & Chakin, I.K. (2024). Efficiency of liquid-phase synthesis of ceramic materials under the influence of an electron beam with high penetrating power. *Bulletin of the University of Karaganda – Physics*, *29*(4(116)), 35–45. DOI: 10.31489/2024PH4/35-45.

22 Zheng, Y., Zou, M., Zhang, W., Yi, D., Lan, J., Nan, C.-W., & Lin, Y.-H. (2021). Electrical and thermal transport behaviours of high-entropy perovskite thermoelectric oxides. *Journal of Advanced Ceramics, 10*(2), 377–384. DOI: 10.1007/s40145-021-0462-5.

С.А. Гынгазов, И.П. Васильев, В.А. Болтуева,
С. Бобуёк, И.К. Чакин, В.П. Кривобоков

Электронды өңдеудің бастапқы реагенттер ұнтақ қоспасының жоғары энтропиялы керамиканың $(Ca_{0.2}Sr_{0.2}Ba_{0.2}Pb_{0.2}La_{0.2})TiO_3$ күйдірілуіне әсері

Термоэлектрлік материалдардың дамуы жоғары энтропиялық материалдардың жаңа класының пайда болуына байланысты белсенді түрде жүргізілуде. Оларды өндіру процестері қатты фазалық синтезге дейін азаяды және реагенттердің ұнтақ қоспаларын механикалық араластырудың ұзақ циклдерін, жоғары температурада термиялық өңдеуді, осы операцияларды бірнеше рет қайталауды қамтиды. Жұмыста электронды-сәулелік өңдеуді қолдану арқылы термоэлектрлік қосымшалар үшін жоғары энтропинді керамика жасау процесін жеделдету мәселелері туралы айтылған. Жоғары энтропиялық перовскит керамикасын $(Ca_{0.2}Sr_{0.2}Ba_{0.2}Pb_{0.2}La_{0.2})TiO_3$ алу мысалында бастапқы реагенттердің ұнтақ қоспасын ауада жоғары энергиялы электронды сәулемен (E = 1,4 МэВ) циклдік өңдеудің керамиканың күйдіру (спекание) процесіне әсері зерттелді. Электронды сәуле тогы 4 мА (5 өңдеу циклі) және 5 мА-дан (4 өңдеу циклі) құрады. Әрбір сәулелендіру кезеңінен кейін ұнтақ механикалық түрде ұнтақталды. Электронды сәуле мен өңдеу күйдіру/тығыздау кинетикасын күшейтеді. Өңдеудің тиімділігі циклдар санымен артады, бұл керамиканың тығыздалу процесін жеделдетеді. Нәтижесінде керамиканың тығыздығы мен механикалық беріктігі жоғарылайды. Бұл жақсартулар электронды сәулемен өңдеу нәтижесінде ұнтақ қоспасында жоғары энтропиялық фаза $(Ca_{0.2}Sr_{0.2}Ba_{0.2}Pb_{0.2}La_{0.2})TiO_3$ түзілуімен байланысты.

Кілт сөздер: жоғары энтропиялық керамика, перовскиттер, синтез, электронды сәулелер, күйдіру

С.А. Гынгазов, И.П. Васильев, В.А. Болтуева,
С. Бобуёк, И.К. Чакин, В.П. Кривобоков

Влияние электронной обработки порошковой смеси исходных реагентов на спекание высокоэнтропийной керамики $(Ca_{0.2}Sr_{0.2}Ba_{0.2}Pb_{0.2}La_{0.2})TiO_3$

Развитие термоэлектрических материалов идет активно в связи с появлением нового класса высокоэнтропийных материалов. Процессы их производства сводятся к твердофазному синтезу и включают длительные циклы механического перемешивания порошковых смесей реагентов, термической обработки при высокой температуре, повторение данных операций несколько раз. В работе решаются вопросы ускорения процесса изготовления высокоэнтропийной керамики для термоэлектрических приложений за счет применения электронно-лучевой обработки. Изучено влияние циклической обработки порошковой смеси исходных реагентов на воздухе с помощью пучка высокоэнергетических электронов (E = 1,4 МэВ) на процесс спекания компактов на примере высокоэнтропийной перовскитной керамики $(Ca_{0.2}Sr_{0.2}Ba_{0.2}Pb_{0.2}La_{0.2})TiO_3$. Ток электронного пучка составлял 4 мА (5 циклов обработки) и 5 мА (4 цикла обработки), при этом после каждого этапа облучения проводилось механическое измельчение порошка. Было установлено, что обработка электронным пучком ускоряет кинетику уплотнения/спекания. Эффективность обработки возрастает с увеличением числа циклов. Это приводит к ускорению процесса спекания, увеличению плотности и механической прочности керамики. Данные улучшения объясняются формированием в порошковой смеси высокоэнтропийной фазы $(Ca_{0.2}Sr_{0.2}Ba_{0.2}Pb_{0.2}La_{0.2})TiO_3$ в результате обработки электронным пучком.

Ключевые слова: высокоэнтропийная керамика, перовскиты, синтез, электронные пучки, спекание

Information about the authors

Ghyngazov, Sergei (*corresponding author*) — Doctor of Engineering Sciences, Leading Researcher, National Research Tomsk Polytechnic University, Tomsk, Russia; e-mail: ghyngazov@tpu.ru, ORCID ID: https://orcid.org/0000-0002-2524-9238

Vasil'ev, Ivan — PhD in Engineering Sciences, Researcher, National Research Tomsk Polytechnic University, Tomsk, Russia; e-mail: zarkvon@tpu.ru, ORCID ID: https://orcid.org/0000-0002-4077-7012

Boltueva, Valeria — PhD in Engineering Sciences, Researcher, National Research Tomsk Polytechnic University, Tomsk, Russia; e-mail: kostenkova@tpu.ru, ORCID ID: https://orcid.org/0000-0001-8128-9042

Bobuyok, Sergei — Engineer, National Research Tomsk Polytechnic University, Tomsk, Russia; e-mail: bobuyok@tpu.ru, ORCID ID: https://orcid.org/0000-0002-9838-1934

Chakin, Ivan — Engineer, Budker Institute of Nuclear Physics SB RAS, Novosibirsk, Russia; e-mail: chak_in2003@bk.ru, ORCID ID: https://orcid.org/0000-0003-0529-2017

Krivobokov, Valery — Professor, Doctor of Physical and Mathematical Sciences, Head of Department, National Research Tomsk Polytechnic University, Tomsk, Russia; e-mail: krivobokov@tpu.ru, ORCID ID: https://orcid.org/0000-0003-0569-3291